Chapter 23
Manganese Emissions From Steelmaking

Donghui Li, Jack Young, Sina Mostaghel, and Kinnor Chattopadhyay

Abstract Manganese emission from pyrometallurgical furnaces is becoming an important issue with more and more stringent environmental restrictions on hazardous air pollutant (HAP) metals across the globe. Manganese is going to become the next pollutant in focus from 2016 onward. Mn emission from steelmaking or ferromanganese furnaces mainly depend on factors such as input load, gas flow rate, blowing practice, and finally the operating conditions of the dust capture systems which control particulate matter emissions. In the present study, several mechanisms of dust formation have been reviewed, and a manganese mass balance was performed to understand the distribution of Mn between liquid metal, slag, and dust for a few BOFs in operation. Operational parameters such as oxygen flow rate, blowing time, hot metal (HM) Mn content, scrap Mn content, end blow Mn%, and conditions of the electrostatic precipitator (ESP) were considered and correlated to plant measurements of Mn emission. Issues related to emissions from EAFs, ferromanganese furnaces, and high-Mn steels have been discussed as well.

Nomenclature

ESP	Electrostatic precipitator
HAP	Hazardous air pollutant
HM	Hot metal
LCA	Lifecycle assessment
LMF	Ladle metallurgical furnace
LRF	Ladle refining furnace
PM	Particulate matter

D. Li • K. Chattopadhyay (✉)
Department of Materials Science and Engineering, Process Metallurgy and Modeling Group (PM2G), University of Toronto, Toronto, ON, Canada, M5S3E4
e-mail: donghui.li@utoronto.ca; Kinnor.chattopadhyay@utoronto.ca

J. Young • S. Mostaghel
HATCH Ltd, 2800 Speakman Drive, Mississauga, ON, Canada, L5K2R7
e-mail: JYoung@hatch.ca; SMostaghel@hatch.ca

23.1 Introduction

Manganese emission to the environment is becoming a major concern for all environmental regulatory bodies around the world, and stringent limits are being imposed. Manganese is among the trace elements least toxic to mammals; however, exposure to abnormally high concentrations, resulting from anthropogenic sources, has resulted in adverse human health effects related to neurotoxicity and may be possible reprotoxicity. Manganese poisoning is characterized by progressive deterioration of the central nervous system, sometimes accompanied by unrelated pneumonitis. The majority of cases have been associated with the breathing of manganese dust or fumes from mining and metallurgical operations. An outbreak of a form of pneumonia in inhabitants of Sauda, Norway, was attributed to manganese emissions from a ferromanganese furnace. Absorption via the gastrointestinal tract and through the skin has also been reported. An outbreak of manganese poisoning in Japan was attributed to ingestion of manganese-contaminated well water. In the early stages of poisoning, removal of the victim from the polluted environment usually clears up manganese; however, in chronic cases, the effects on the central nervous system are not completely reversible. Exposure to high concentrations of Mn may lead to Parkinson disease.

On the review of literature and environmental guidelines from different countries, it was found that the permit limits are very different in each country, and in most cases a local municipal permit limit applies which overrules the federal standards. Table 23.1 introduces some permit limits of manganese in air around the world. The USA has the strictest limit on manganese emissions in air.

The principal sources of ambient environmental pollution by manganese are emissions from metallurgical processing plants and reprocessing waste materials. Emissions to the atmosphere from industrial plants and processes will vary considerably, depending upon the process involved and the degree of control exercised. Manganese has been found in measurable amounts in practically all samples of suspended particulate matter collected by the National Air Surveillance Networks (NASN) from the air of some 300 urban areas. The highest concentrations, as expected, are found in the vicinity of ferromanganese alloy plants or related activities. The NASN urban average manganese concentration is less than 0.2 microgram per cubic meter ($\mu g/m^3$), but several cities have annual averages in the 0.5–3.3 $\mu g/m^3$ range. Occasional 24-hour concentrations as high as 14.0×10^3 $\mu g/m^3$ have been measured. Annual averages as high as 8.3 $\mu g/m^3$ have occurred in small communities located near a large point source in the highly industrialized Kanawha River Valley of West Virginia. In Norway, concentrations of over 46 $\mu g/m^3$ have been reported in the vicinity of a ferromanganese plant. Approximately 80 % of manganese in the suspended particulate matter from six large cities in the USA was associated with particles in the respirable size range—that is, 5 μm or less in diameter. The existence of manganese in the smaller particles favors a widespread distribution of this pollutant. Such distribution has been confirmed by the analysis of precipitation samples collected at many remote locations in the USA (Singh 2005; Vasu 2006).

It has been estimated that over 80 % of the total national manganese emissions in 1968 was from iron, steel, and ferroalloy production. Dust from the handling of raw materials in metallurgical processing and other production activities, such as the manufacture of chemicals, fertilizers, fungicides, and dry cell batteries, may result in local manganese pollution problems (1975). Table 23.2 shows the Mn emission factors for various ferrous and ferroalloy processes.

Table 23.1 Review of some permit limits of manganese in air around the world

Country	Regulatory body	Type	Element	Description of the limit	Value
Canada	Health Canada	Air	Manganese	Reference concentration to which the population could be exposed for a lifetime without appreciable risk of adverse health effects	0.11 µg/m³
USA	Environmental Protection Agency (EPA)	Air	Manganese	Reference concentration	0.05 µg/m³
Global	World Health Organization (WHO)	Air	Manganese	Recommended air quality guideline values—TWA—for individual substances based on effects other than cancer or odor/annoyance using an averaging time of 1 year (annual)	0.15 µg/m³

Table 23.2 Mn emission factors for various ferrous and ferroalloy processes (Singh 2005)

Process	Factor	Unit
Mining	0.09	kg/ton of Mn ore mined
Mn metal	11.36	kg/ton of Mn processed
Mn blast furnace	10.86	kg/ton of FeMn produced
Si-Mn	31.55	kg/ton of SiMn produced
Ironmaking blast furnace	10.22	kg/1000 tons of hot metal produced
BOF	35.45	kg/1000 tons of steel produced
Electric furnace	35.45	kg/1000 tons of steel produced
Welding rods	7.27	kg/ton of Mn processed
Nonferrous alloys	5.45	kg/ton of Mn processed
Batteries	4.54	kg/ton of Mn processed
Chemicals	4.54	kg/ton of Mn processed
Coal	3.5	kg/ton of coal burned

Emissions from oxygen steelmaking furnaces are in the form of solid filterable particulate matter and condensable gasses. One of the largest sources of filterable particulate matter (PM) and hazardous air pollutant (HAP) metals is the BOF electrostatic precipitator (ESP) during the oxygen blowing period, and a feasible option for reducing these emissions is to upgrade the ESPs to improve emission control performance. Consequently, reducing the filterable PM emissions from these sources would result in co-control of HAP metals. Feasible controls have been demonstrated at several steel mills in North America, Europe, and Japan. These mills use hoods exhausted to bag houses to capture emissions that occur when the blast furnace is tapped and when the BOF is charged and tapped. An efficiently designed and operated fume control system can achieve a reduction of 95 % or more (from the uncontrolled case) in HAP metal emissions from these sources. Review of historical test data suggests that, if variability in operating parameters is minimized and if the ESPs perform consistently at their lowest measured emission rates, emissions could be reduced by 50 % or more from current operating levels.

Manganese has been listed as one of the top hazardous air pollutant (HAP) metals by environmental regulatory boards in Europe and North America. In a recent report by RTI international (Vasu 2006), it is seen that in the Detroit area, manganese tops the list among all HAP metals at 13 t per year with much lesser quantities of nickel, chromium, and lead. Table 23.3 shows the exact numbers. Because of the high temperatures of steelmaking operations (1600 °C), the more volatile metals are removed and concentrated in the PM. The primary metal HAP is manganese, which was reported in an EPA survey as about 1 % of the BOF dust. Other analyses of BOF dust averaged 1.1 % manganese, 0.74 % lead, 0.03 % chromium, and 0.01 % nickel. BOF slag contains about 4.3 % manganese, 0.001 % each lead and nickel, and 0.1 % chromium.

23.2 Theoretical Considerations

23.2.1 Mechanisms of Dust Formation During Steelmaking

There are several hypotheses for the mechanism of dust formation in basic oxygen furnaces (BOFs). They are direct hot metal vaporization, hot metal/slag ejection by CO bubble bursting, metal/slag ejection by mechanical action of the impinging

Table 23.3 Total HAP metals emissions from two steel works and one coke battery

HAP metal	Total emissions ton/year	HAP in $PM_{2.5}$ ton/year
Mn	13	7.2
Pb	1.9	0.7
Ni	0.04	0.01
Cr	0.2	0.1
Hg	0.4	0.4
Total	15.5	8.4

oxygen jet, and entrainment of solid particles during top charging. It is difficult to say which is the dominant mechanism, but studies indicate that the mechanism changes during the blow time. Vaporization typically occurs due to local hot spots that are generated by highly exothermic reactions during oxygen blowing in the BOF process. Various studies indicated that the local hot spot temperature could be in the range of 2100–3050 °C (Goetz 1980). When fume particles are formed entirely by the condensation of vapors, then the highly volatile elements (e.g., Mn) get enriched in the fume. In the temperature range of 1400–2100 °C, the vapor pressure of Mn is 100–1000 times higher than that of iron; hence, analyses of fumes produced solely due to vaporization show Mn/Fe ratios in the order of 30–150 times compared to the Mn/Fe ratio in the bath. The dust particles formed as a result of the vaporization mechanism can be identified by their octagonal ($FeFe_2O_4$) or rhombo-hedral (Fe_2O_3) shape.

The other mechanism is dust formation by hot metal/slag ejection by CO bubble bursting or mechanical action of the impinging jet. In either case, the dust particles are spherical in shape. Also, the Mn/Fe ratio in the fume is almost equal to the Mn/Fe ratio in the bath as there is no vaporization involved. In reality, BOF dust is formed by a combination of both mechanisms and that can be tracked by plotting the Mn/Fe ratio in fume to the Mn/Fe ratio in bath with blowing time. Goetz (1980) in his studies indicated that large ratios imply a mechanism of direct vaporization, whereas a low ratio indicates metal/slag ejection as the mechanism of dust forma-tion. Figure 23.1 shows a typical Mn/Fe ratio plot with blowing time.

Evidently, metal/slag ejection by CO bubble bursting or mechanical action is the dominant mechanism of dust formation at the beginning of the blow. However, toward the end of the blow, vaporization becomes more dominant. This finding of 1980 was also reconfirmed by Tsujino et al. (1989) in 1989, Nedar (1996) in 1996, and Gritzan and Neuschutz in 2001. Nedar also concluded that 60–70 % of the dust
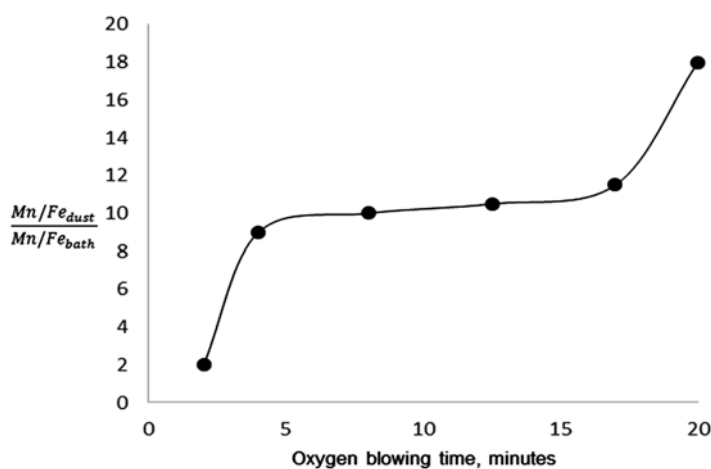

Fig. 23.1 Variation of Mn/Fe ratio of the dust over that of the bath with blowing time

is formed by metal/slag ejection (bubble bursting) mechanism, whereas other mechanisms contribute to the rest 30 %. Gritzan and Neuschutz (2001) also advocated for metal/slag ejections to be the primary mechanism for dust generation in BOF operations.

Based on Mn/Fe ratios, Goetz (1980) summarized that the amount of BOF dust generated by vaporization mechanism during the decarburization period is about 1.8 % by weight, whereas the degree of vaporization during preignition and re-blow is about 10 %. So it can be concluded that direct vaporization during the re-blow and preignition periods is about five times larger than that during decarburization period of the blow. However, the major mechanism of fume formation remains that of metal/slag ejection and bubble bursting.

Another probable cause of dust generation is top charging of lime during the blowing period. However, it is seen that top charging increases the dust generation rate only momentarily, i.e., it only affects the instantaneous dust generation rate and not on the total amount of dust generated. The possible reason for momentary increase in dust generation rate during top charging is because the slag layer collapses due to solid lumps falling upon the slag. On the other hand, the early period of lime charging takes place before the slag starts to foam, and it is during this period that the increase in dust generation is particularly strong. Also, the top charged material are usually rough surfaced solid lumps which act as nucleation sites for CO bubbles and enhances bubble bursting and dust generation momentarily. Goetz, in his thesis, also discussed the effect of bath temperature and bath carbon content on fuming rates in a BOF. For a fixed carbon content, the lower the bath temperature (lower the superheat), the greater the metal/slag ejection and hence higher the fume rate. Lower bath temperatures also result in lower slag temperature and higher slag viscosities, which impedes the formation of a stable foamy slag cover and helps in entrapping a part of the metal ejections. This also results in higher fume rates. It can also be inferred that all parameters which contribute to stable foaming in the slag can reduce the dust emission rates from the furnace. Based on the extensive research effort conducted by Fruehan and his team (1995), a higher viscosity and lower density and surface tension of the slag lead to formation of foams with more height, which are also more stable and last longer, hence reducing the emission rates from the furnace.

The dust generation rate in the BOF decreases rapidly with blowing time. Goetz showed some typical curves (Fig. 23.2) to represent dust generation rate versus blowing time in an experimental BOF.

The general trend of a decreasing dust generation rate with blow time was confirmed in all cases of normal practice, and this phenomenon has been repeatedly reported in literature (Gritzan and Neuschutz 2001) (Figs. 23.3 and 23.4).

Figure 23.5 shows the dust generation rate as a function of top-blown oxygen flow rate during the middle stages of the blowing (one fourth to three fourth blowing period) in a 250 and 300 t BOF with combined blowing practices (Tsujino et al. 1989). Higher flow rates of oxygen results in increased dust generation rate.

There is a direct relation between the dust generation rate and carbon content of the melt and this has been reported by several investigators (Knaggs and Slater
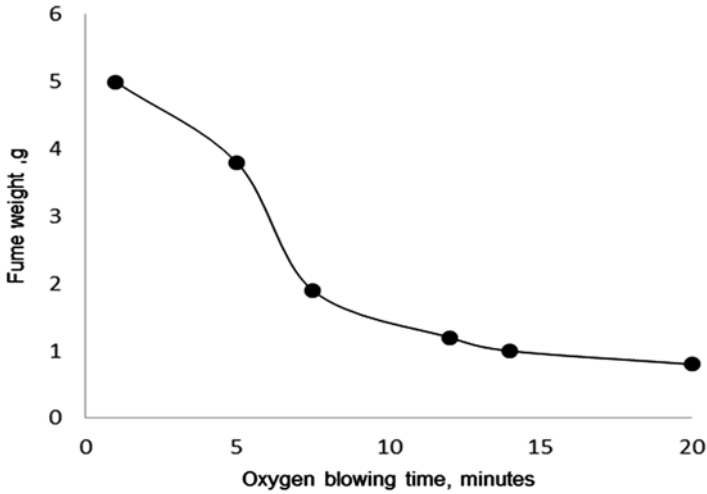
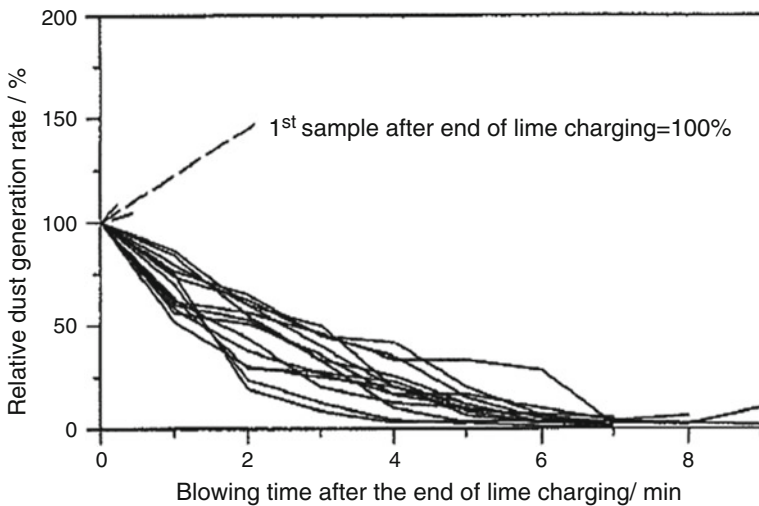**Fig. 23.2** Fume weight versus blowing time (Goetz 1980)

Fig. 23.3 Relative dust generation rate versus blowing time in a 200 t BOF at ThyssenKrupp Dortmund (oxygen flow rate was constant throughout the blow period)

1959; Turkdogan and Leake 1959; Ellis and Glover 1971; Ohno et al. 1986; Herwig 1995). In fact, the only variable that changes with blow time is the carbon content of the bath. Gritzan and Neuschutz (2001) based on their observations explained the steady decrease of dust generation rate with blowing time in a BOF. At the beginning of the blow, due to high momentum and velocity of the oxygen jet impinging on the melt surface, large quantity of splashes are formed and ejected into the gas atmosphere above the melt. The droplets are greater than 10 mm, i.e., much larger
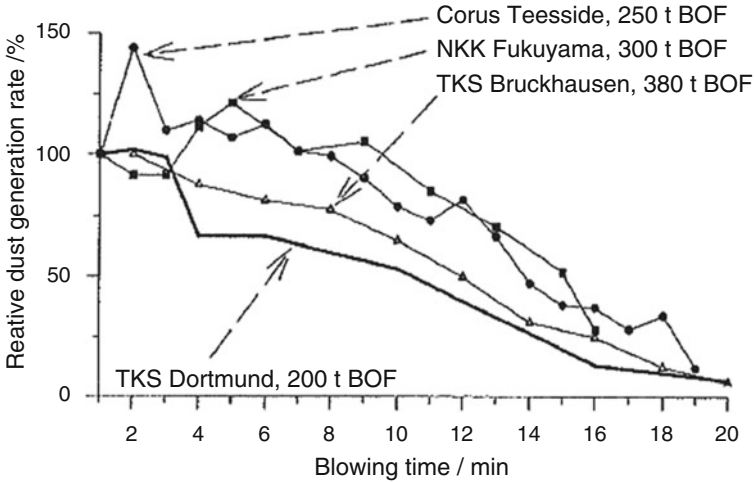
Fig. 23.4 Relative dust generation rate versus blowing time for different vessel sizes (oxygen flow rate was constant throughout the blow period)
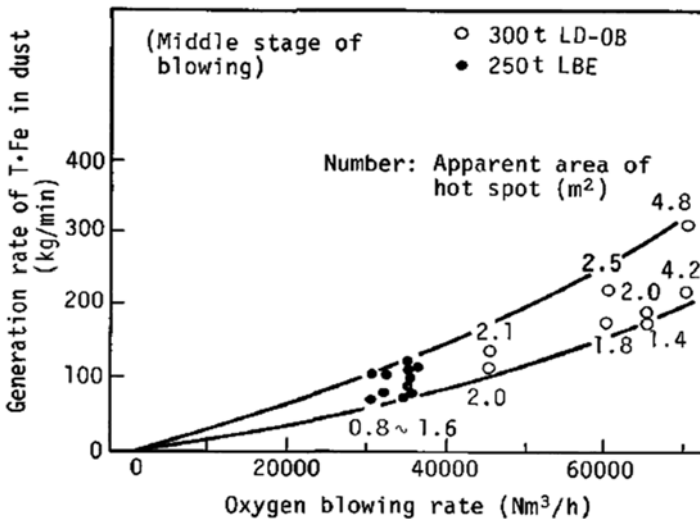

Fig. 23.5 The dust generation rate as a function of top-blown oxygen flow rate during the middle stages of the blowing (one fourth to three fourth blowing period; combined blowing was performed)

than dust particles. Most of the splashes/droplets return back to the melt after a parabolic flight. As long as they contain sufficient carbon, their liquidus temperature is relatively low, and so they remain liquid during the entire flight time. In that state, the droplets rapidly dissolve oxygen, which reacts with carbon to form CO bubbles inside the droplets/splashes. The CO bubbles rise to the splash surface, burst, and

form smaller film and jet droplets, which are immediately carried away by the off-gas. Now the liquidus/solidus temperatures of these splashes will rise steadily with blow time as the carbon content of the melt decreases. With lower carbon content the formation of a solid shell around the splash starts earlier in its flight above the bath. Then, the rapid dissolution of oxygen into the liquid splashes is restricted to a shorter period of time. This reduces the overall dust generation rate. With increasing blowing time, a stable layer of slag forms on the top surface of the melt, which also entraps most of the droplets formed by CO bubble bursting. Therefore, the overall, dust generation rate decreases with blow time.

23.2.2   Size Distribution and Chemistry

Since this chapter's focus is on manganese, the dust chemistry was reviewed in terms of Mn, MnO, and Mn/Fe ratio content in BOF dust. Some observations were also reported on dust particle size range and its relationship to dust chemistry. Goetz (1980) reported on dust chemistry from industrial BOFs. The fume particles that result from vaporization are either hexagonal or octagonal in shape and exist over a limited size range of 0.05–0.2 μm in diameter. Fumes resulting from vaporization also have a very high concentration of volatile elements like Mn (50–150 times) than the bulk bath from which it originated. On the other hand, the dust particles which are formed by the process of metal spray/ejection are spherical in shape and exist over a larger size range from 0.05 to 5 μm in diameter. In these dust/fumes, the concentration of Mn is the same as that in the bulk. Krichevtsov (1970) reported on the evolution of fume chemistry with blowing time. From Krichevtsov's calculations, the average Mn/Fe ratio in the fume is around 0.033. In a BOF, the majority of the manganese is oxidized in the first few minutes of the blow, and then the Mn level in the bath ranges between 0.15 and 0.3 depending on the initial hot metal Mn content. Assuming the Fe content of the bath greater than 95 %, the Mn/Fe ratio in the bath is 10–15 times lower than that in the fume. From Krichevtsov's results, the calculated Mn content of the fume ranges between 0.9 and 3.3 %. These calculations were used and the evolution of Mn content in the dust with blow time is plotted in Fig. 23.6. It is clearly seen that the Mn content in the dust is not constant and varies along the blow period. The major chemical components of BOF dust are (FeO_x), CaO, MgO, and MnO.

Nedar (1996) reported on dust chemistry based on his tests on a 100 t BOF operation at SSAB Tunnplat AB, in Luleå, Sweden. He showed that Mn levels vary significantly in the two stages of the blow. The first part of the blow was for 7 min, while the second part lasted for another 6–10 min.

From a previous study by Laciak (1977) based on an operation at ArcelorMittal Dofasco, the Mn% in the fume versus blow time was also plotted and is shown Fig. 23.7. Average Mn/Fe ratio in the fume is 0.46/61.7 = 0.007, whereas for the second part of the blow, it is 1.16/66.9 = 0.017 which is almost 2.5 times higher. So the dust is enriched with manganese in the second stage of the blow.
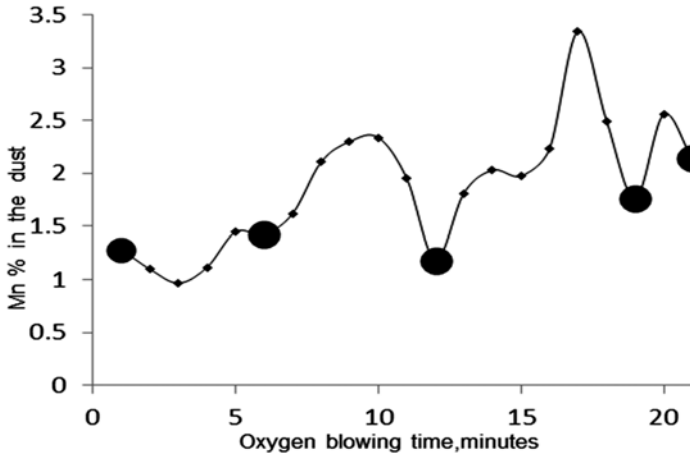
Fig. 23.6 Variation of Mn% in BOF dust with blowing time (the *black circles* are the times at which lime were added)
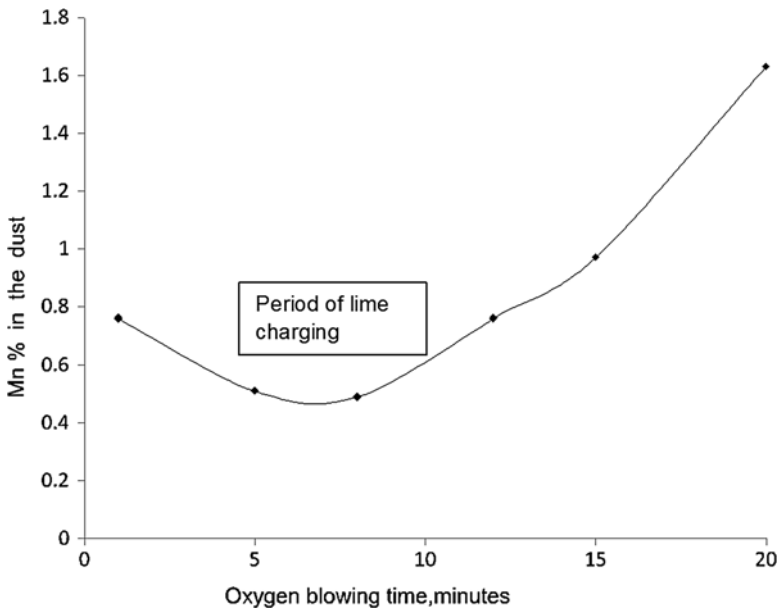

Fig. 23.7 Variation of Mn% in BOF dust with blowing time

Gritzan and Neuschutz (2001) reported on dust size and chemistry from their studies on a 200 t BOF operating at ThyssenKrupp, Dortmund. The Mn content of the dust varies between 0.077 and 0.38 wt%. A typical size distribution of the dust particles is shown in Fig. 23.8. The observed size distribution breaks down to four distinct classes with their individual maxima at 1, 12, 50, and 140 μm. The particle size distribution did not vary significantly with blowing time or with top charging.
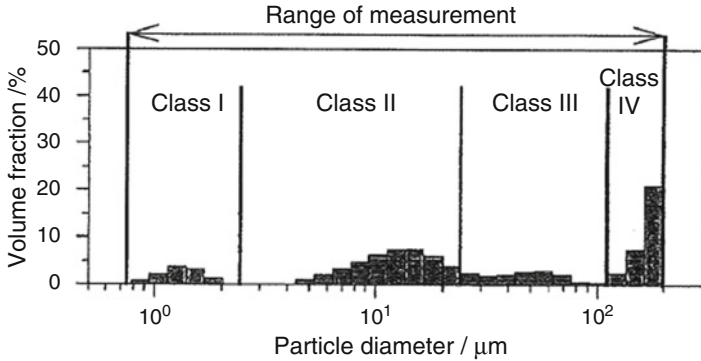
Fig. 23.8 Particle size distribution from the dust samples as reported by Gritzan and Neuschutz (2001)
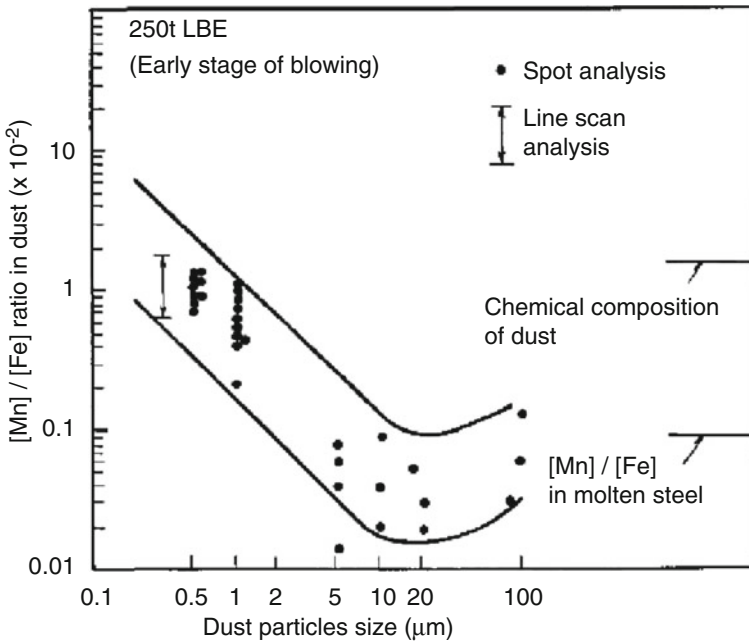

Fig. 23.9 Relation between Mn/Fe ratio in the dust and dust particle size (early stage of blowing)

Tsujino et al. (1989) reported on dust composition and size range from their studies in 175, 250, and 300 t BOFs with minimum slag practice. Figures 23.9 and 23.10 show the Mn/Fe ratio in the dust versus particle size for the early stages of blow and the end of the blow, respectively. When the dust particle size is as fine as 5 µm or less, the smaller the dust particle size, the higher is the Mn/Fe ratio. The Mn/Fe ratio in dust whose particle size is 1 µm or less is about 5–20 times as much as that in the
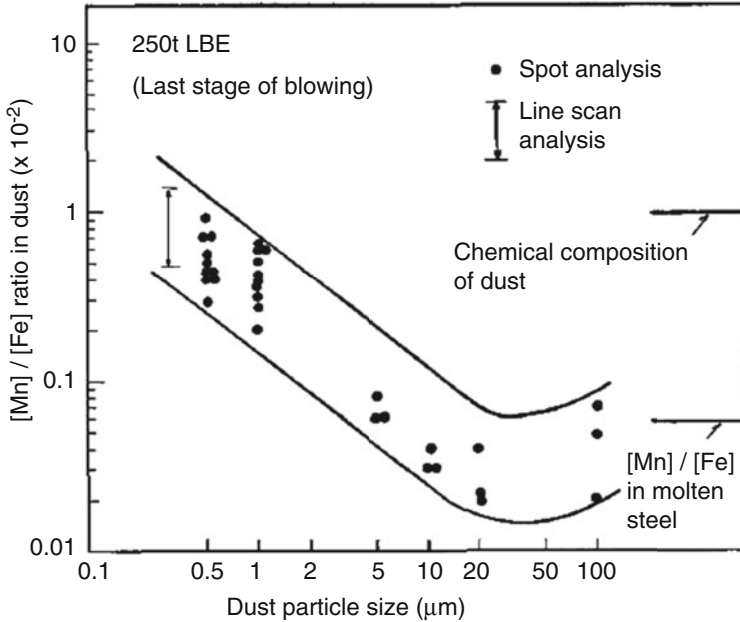
Fig. 23.10 Relation between Mn/Fe ratio in the dust and dust particle size (later stage of blowing)

melt. Also, with respect to dust having particle size of 5–10 μm, the Mn/Fe ratio in dust is lower than that in the bath, which is minimum for all particle sizes. When the particle size becomes larger, the Mn/Fe ratio in dust is approximately equal to that of the bath. At any dust generation rate, the smaller the dust particle size, the higher the concentration of Mn in the dust.

23.2.3 Factors Affecting End Blow Mn Content

The major operational parameters that influence the end blow manganese behavior in the BOF are hot metal manganese input, slag volume, oxidation level, and temperature (Dias Barao et al. 2008). Manganese oxidation in the BOF occurs by either direct oxygen or by indirect oxidation via FeO. The manganese oxidation reaction is exothermic implying lower equilibrium constant values with increasing temperatures. So from a thermodynamic point of view, higher temperatures would lead to larger amounts of Mn recovery. However, manganese recovery is also affected by dissolved oxygen content. At the end of the blow, dissolved oxygen content is higher, and this leads to manganese oxidation. Manganese oxidation is mainly dictated by lower temperatures, increasing FeO content and increasing the activity coefficients ratio of FeO and MnO. For a given slag composition and a known blow

temperature profile, the theoretical manganese partition can be calculated at every instant during the blow. Figure 23.11 shows the variation of Mn partition with blowing time. It shows a good degree of fitting starting from the second period of blowing (approximately at 40 %, when the oxygen lance height is increased, and the oxygen flow rate is reduced), meaning that from this moment on, the manganese oxidation is controlled by slag/metal reaction and FeO oxidation. Figure 23.12 shows the relationship between hot metal Mn content and end blow Mn concentration from data collected from ten steel plants in Brazil. There is definitely an increase
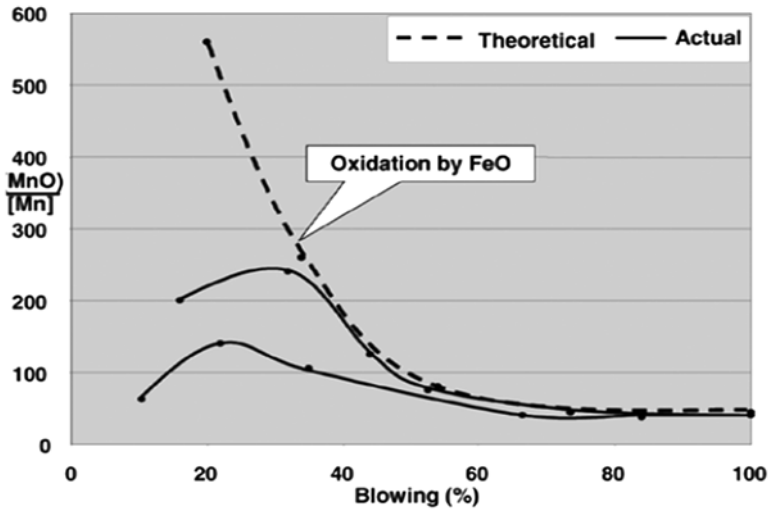

Fig. 23.11 Variation of Mn partition with blowing time (linear time dependence of temperature was assumed)
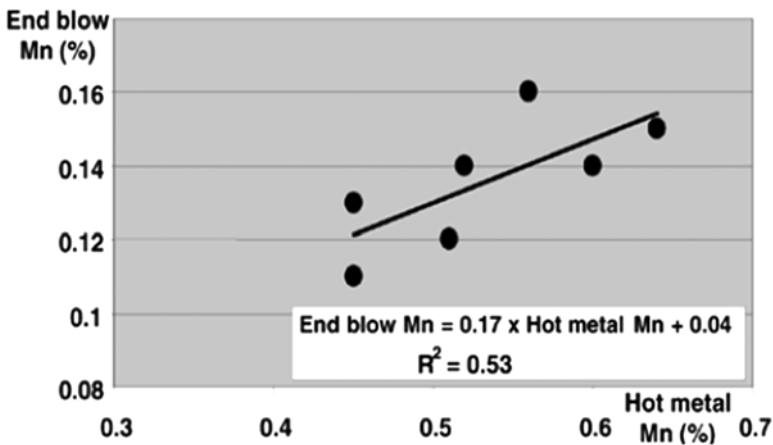

Fig. 23.12 Hot metal Mn concentration versus end blow Mn content

in end blow manganese concentration if hot metal Mn content is high. It is evident that only a small fraction (17%) of the hot metal manganese is recovered in the steel. The influence of hot metal Mn content on end blow Mn is higher at higher carbon contents. The slag/metal manganese partition ratio decreases for increasing hot metal manganese content. The higher the temperature, the smaller the slag/metal manganese partition ratio; this effect adds up to the effect of hot metal manganese content. The effect of hot metal Si on end blow Mn is not disturbed by the oxidation level, and it is lesser than the effect of hot metal Mn content. Several factors that influence the Mn partition between slag and metal are FeO and CaF_2 contents of the slag, and temperature (Jung et al. 2002). The Mn distribution ratio increases with FeO content linearly in the FeO concentration range of (6–25 mass %). The Mn partition ratio decreases with increasing CaF_2 content in the slag. However, most plants do not use CaF_2 due to the environmental issues.

Detailed data analysis was performed at a BOF shop in North America with two BOFs in operation, and similar trends on end blow Mn were observed. The results are presented in Fig. 23.13 (Chattopadhyay et al.).

23.3 Results and Discussion

23.3.1 Mn Emissions From BOFs

One of the major reasons for increased focus on Mn is the quality of the raw materials including iron ore pellets and scrap. The BOFs are usually receiving higher Mn hot metal than before, and this is obviously related to high-Mn hot metal production
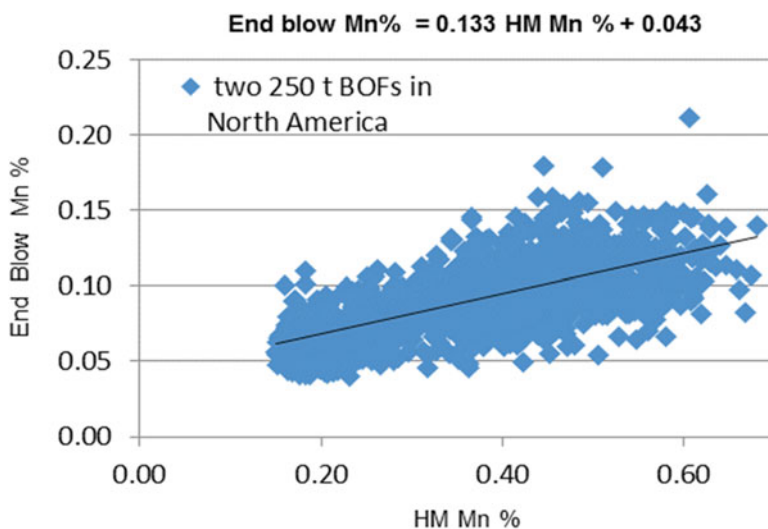
Fig. 23.13 Manganese concentration in the end blow as a function of hot metal Mn content for two North American BOFs

at the blast furnaces. As the iron ore mines are digging deeper and deeper into the earth's crust, the Mn content of the ore keeps on increasing. Figure 23.14 shows the trend for an iron ore mine in North America.

Plants operate with varying levels of hot metal Mn (AIST 2012), and this is illustrated in Fig. 23.15. HM Mn concentration can range between 0.2 and 1.0 wt% and depending on the Mn input load, the amount of Mn in the dust and fumes will be affected based on the partition ratio. Some data from steel plants were considered for the Mn mass balance analysis and the details are shown in Table 23.4. The mass balance was performed based on plant data, including steel and slag analysis and ESP dust analysis and stack test data. It is clear from Table 23.5 that for BOFs, 25–28 % of the Mn goes into the liquid steel, 69–71 % into the slag as MnO, and
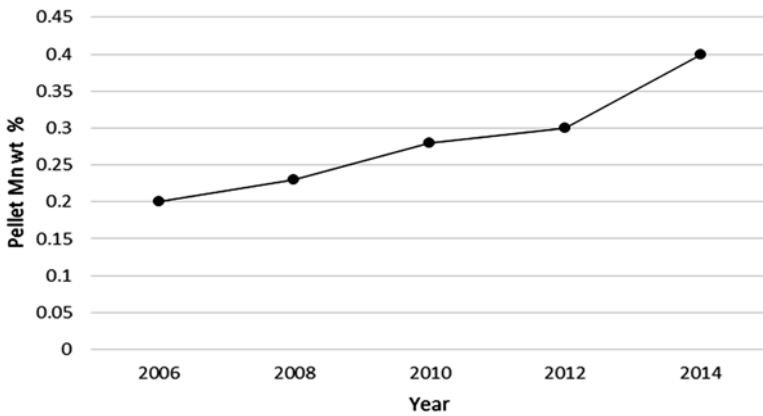

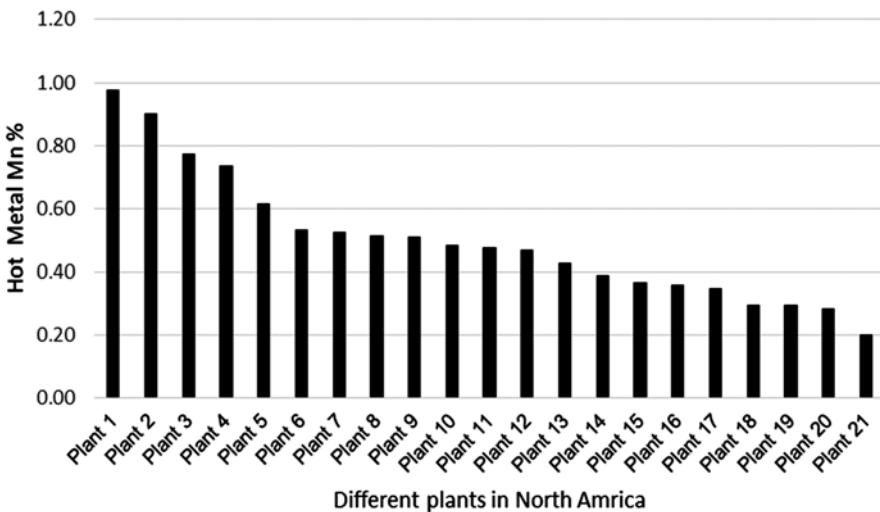**Fig. 23.14** Increase in Mn content of the pellets over the past decade

Fig. 23.15 Different levels of Mn in hot metal (AIST 2012)

Table 23.4 Manganese concentration in hot metal for plants considered

	HM Mn wt%
Range for BOFs in North America	0.2–1 %
Range for BOFs in Brazil	0.4–0.7

Table 23.5 The distribution of Mn among liquid steel, slag, and dust/fumes

	% of Mn in *outputs*		
	Liquid steel	slag	dust
Average of two BOFs in North America	28	69	3
Average of BOFs in Brazil	25	71	4

Table 23.6 PM and Mn emission rates from different ESPs

	Mn kg/h	Permit limit kg/h	PM in kg/h	PM permit limit kg/h
ESP with minimal maintenance	0.15	0.046	10	23
Upgraded ESP	0.06	0.046	6	23
Upgraded and well maintained ESP	0.04	0.046	3.5	23

Table 23.7 HM Mn % versus dust Mn %

HM Mn wt%	Dust Mn wt%	Ratio
0.28	0.45	1.61
0.44	0.68	1.55
0.45	0.83	1.84
0.49	0.86	1.76
0.52	0.90	1.73

3–4 % goes into the dust. Of course these partition ratios vary depending on the furnace operating conditions including temperature and partial pressure of oxygen. Considering the highly oxidizing nature in BOF furnaces, it is expected to have more Mn in the slag.

About 3–4 % of Mn goes into the dust for BOFs, most of the dust should be captured by the ESP system. A good ESP that is well maintained can easily prevent Mn emissions by capturing most of the solid dust particles. Data was collected from a steel plant and PM and Mn emission rates (kg/h) were correlated with ESP operating condition. A summary of which is presented in Table 23.6.

Table 23.7 shows the ratio between the Mn% in the dust to the hot metal Mn%, and the ratio is fairly constant for various hot metal Mn levels. It ranges between 1.5 and 1.9.

23.3.2   Manganese Emission From High Mn Steels and Other Pyrometallurgical Processes

Most steel grades contain only about 0.5–1.0 % manganese, which as discussed above by itself is a safety and environmental concern. Obviously, production of Mn-rich ferroalloys (i.e., ferromanganese or silicomanganese) or specialty high-Mn alloys (e.g., twinning induced plasticity (TWIP) or transformation induced plasticity (TRIP) steels) can emit more Mn to the atmosphere (if not controlled).

Recently, Paymandar et al. (2014) have investigated the interfacial reactions between slag and high manganese and aluminum alloy steels between 1500 and 1550 °C. They experimentally measured the manganese loss due to evaporation from four different steel compositions: V1, 17%Mn-1.5%Al; V2, 22%Mn-1.5%Al; V3, 22%Mn-3%Al; and V4, 17%Mn-3%Al. They have concluded that the total manganese loss from these steels can be between 0.59 and 1.8 % of the total manganese content (Fig. 23.16), which is significant and necessarily needs to be controlled.

Emission of Mn from high-Mn ferroalloys is also a significant concern. High-carbon ferromanganese, which is primarily produced in submerged-arc electric furnaces, contains up to 80 wt-% Mn and 7.5 % carbon. The recovery of Mn in the alloy is about 70–80 %; the remainder reports to slag as MnO or to the off-gas as Mn-containing species. The slag generated during FeMn production may contain as high as 42 wt-% Mn and is used to produce silicomanganese, containing 12.5–18.5 wt-% silicon and ~65–68 wt-% Mn, which will in turn be used for to alloy low-carbon steel.

Hatch and the International Manganese Institute (IMnI) have recently completed the first life cycle assessment (LCA) of global manganese alloy production. The study considered 17 manganese mines and smelters providing a standard measure of average environmental performance for the release of greenhouse gasses, particulate
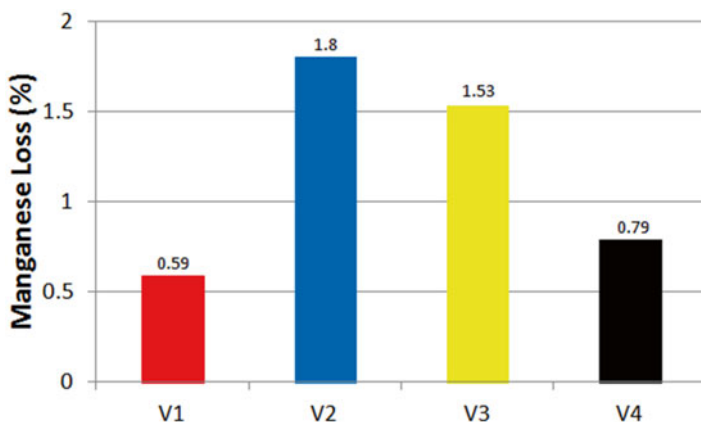

Fig. 23.16 Manganese loss by oxidation and evaporation from different steel compositions

matter (PM), NO_X and SO_X, as well as water and energy consumption and waste generation (Westfall et al. 2015). In this analysis, the LCA supply chain has been grouped into the following categories, which also represent sources of Mn emission:

1. Mineral extraction and hauling.
2. Ore processing, beneficiation, and delivery.
3. Sinter production and delivery.
4. Smelting (furnace production), in all three types of electric arc furnace, i.e., open, semi-open, and sealed. This unit process is the major source of Mn emission. To address this issue, the following controlling equipment have been used:

   - Fabric filters with particulate capturing efficiency of over 99 %
   - High-pressure-drop venturi scrubbers with particulate capturing efficiencies between 94 and 98 %
   - Wet scrubbers, including both multistage centrifugal scrubbers and venture scrubbers, with particulate removal efficiency of 99 %

5. Metal casting, crushing and screening, materials handling, and other auxiliary smelter activities.

The United States Environmental Protection Agency (EPA) (1985) has derived emission factors for ferromanganese production furnaces, assuming an average Mn ore grade of 45 % and production of 80 wt-% Mn FeMn, listed in Table 23.8.

Most of the alloying in steel is done at the LRF, and thus it is important to see the partition ratio of Mn in the LRF. Data was collected from two LRFs in operation at a steel plant in North America. These particular LRFs had a very low oxygen level as Al was added in majority of the heats. Because of low oxygen potential, very little Mn was lost in the slag as MnO. Table 23.9 shows the distribution of Mn in the LRF. It is clearly seen that 99 % of the Mn is retained in the liquid steel, 0.78 % goes into the slag and 0.001 % goes into the dust. The stirring energy and oxygen potential is very little at the LRF when compared to the BOF. As the major mechanism of Mn emissions is by CO bubble bursting and mechanical action, these results are very reasonable.

Table 23.8 Emission factors derived for ferromanganese production furnaces

Source		Mn emission factor kg/ton of ore processed/metal produced
Raw material processing	Receipt and storage of Mn ore	0.45
	Crushing and sizing	0.45
	Weighting and feeding	0.4
Smelting (uncontrolled)	Open furnace	6.6
	Semi-sealed	2.6
	Sealed	9.6

Table 23.9   Distribution of Mn in the ladle refining furnace (LRF)

	Wt (lbs)	Mn%	Wt of Mn (lbs)	% Input
Input				
Incoming steel ladle	506,017	0.21	1,062	60.22
Ferroalloys added	780	90.00	702	39.78
Total Mn input			*1,764*	
Output				
Mn in liquid steel	500,000	0.35	1,750	99.22
Dust	Based on dust generation rate and treatment time		0.02	0.001
Mn going in LRF slag	The balance		13.8	0.78
Total Mn output			*1,764*	

23.3.3   *Manganese Consumption*

The manganese consumption in the steel industry is not projected to increase substantially in the next 10 years, estimated consumption per ton of crude steel will remain at ~7 kg/t. Some new steel grades with higher Mn are being developed; however, it is not anticipated that these products will have a significant impact on the overall Mn consumption rate. There are some other TRIP and TWIP steel grades with Mn levels in excess of 20% which are being developed for small niche products; however, special continuous casters are required to cast such product, and this will not have a significant impact on overall Mn consumption. Overall crude steel production is projected to increase in the next 10 years; the expected annual growth rates in steel are ~3.0% which will ultimately translate into an overall increase in manganese consumption. To put this into perspective, the projected annual increase in crude steel production is 45 million ton per year, which will impact Mn consumption. Increased BOF steel production will increase the consumption of higher Mn-containing iron ores, which can potentially increase the Mn emission levels from the BOF if environmental systems are not maintained properly. However, the majority of the increased Mn associated with this increase in steel production will be in ferroalloys added typically when the steelmaking furnaces are tapping or subsequently at secondary ladle metallurgy facilities (ladle furnaces and vacuum degassers). Emissions associated with these manganese additions should be captured by the secondary emission systems at the steelmaking furnace or with fume capture equipment at the secondary treatment facilities.

23.4   Conclusions

Mn emission is a concern because of its detrimental effects related to neurotoxicity and perhaps reprotoxicity. The steel industry is one of the major sources of Mn emissions, and in today's scenario, the raw materials have more Mn content in them

than before. The higher Mn content in the ore is attributed to the increased amount of Mn in the earth's crust, as it is being mined deeper and deeper. The higher Mn in the ore results in higher Mn in the hot metal which in turn causes the problem of Mn emissions during basic oxygen steelmaking. The dominant mechanism of Mn emission in the BOF is by mechanical action due to the supersonic jet, as well as CO bubble bursting, due to high oxygen potential. The results show that as the hot metal Mn is increased, the Mn in the slag and dust have also increased proportionally. For a BOF, typically 25–30 % Mn is retained in the steel, and 65–70 % goes into the slag, and around 3–4 % goes into the dust. However, it is not a concern as long as the off-gas cleaning systems are well maintained. This study showed that, for an upgraded and well maintained ESP, the stringent permit limits can be achieved.

Emission of Mn from high-Mn ferroalloys is also a significant concern: High-carbon ferromanganese, which is primarily produced in submerged-arc electric furnaces, contains up to 80 wt-% Mn and 7.5 % carbon. The recovery of Mn in the alloy is about 70–80 %; the remainder reports to slag as MnO or to the off-gas as Mn-containing species.

When alloying is performed at the LRF/LMF, the conditions are significantly different. The oxygen potential and the stirring energy at the LRF/LMF are way lower than the BOF, and hence retention of Mn alloy in the steel is almost 99 %, and very little ends up in the emissions. Therefore, for the production of high-Mn steels, majority of the alloying should be performed at the LRF/LMF, resulting in little Mn dust emission.

References

AIST (2012) Internal report, Ironmaking Committee

Chattopadhyay K, Johnson D, Young J, Vieira J, Bachenheimer S, Kumar S (2014) Evaluation of air emissions in steel plants with focus on heavy metals emission. AISTech 2014, Indianapolis

Dias Barao C, da Silva CA, da Silva IA (2008) Analysis of parameters affecting end blow manganese content at oxygen steelmaking. La Reveue de Metallurgie 105:556–561

Ellis AF, Glover J (1971) Mechanism of fume formation in oxygen steelmaking. J Iron Steel Inst 209:593–599

Goetz F (1980) The mechanism of B.O.F. fume formation. Dissertation, McMaster University

Gritzan A, Neuschutz D (2001) Rates and mechanisms of dust generation in oxygen steelmaking. Steel Res 72:324–330

Jung S-M, Rhee C-H, Min D-J (2002) Thermodynamic properties of manganese oxide in BOF slags. ISIJ Int 42:63–70

Knaggs K, Slater JM (1959) Some factors affecting fume evolution in molten steel during oxygen injection. J Iron Steel Inst 193:211–216

Krichevtsov E (1970) Special operating procedures during the blowing of high-phosphorus hot metal in the ld-ac shop at the huckingen works of Mannesmann AG. Stal 2:113–118

Laciak S (1977) A study of the kinetics and mechanisms of materials ejection from a basic oxygen furnace. Dissertation, McMaster University

Nedar L (1996) Dust formation in a BOF converter. Steel Res 67:320–327

Ohno T, Ono H, Okajima M (1986) Pure steel droplet ejection. Trans ISIJ 26:B-312

Paymandar M, Schmuck S, Schweinichen P, Senk D (2014) Interfacial reactions between slag and melt in the new world of high manganese steels. EPD Congress, TMS Annual meeting

Schurmaan E, Polch A, Pfilipsen HD, Herwig U (1995) Chemical-composition, generation mecha-
    nism and formation rate of converter dust. Stahl und Eisen 115:55–61
Scientific and Technical Assessment Report on Manganese (1975) Program Element No. 1 AA001
    ROAP No. 26AAA, US EPA
Singh VP (2005) Toxic metals and environmental issues. Sarup & Sons, New Delhi
Tsujino R, Hiral M, Ohno T, Ishiwata N, Inoshita T (1989) Mechanism of dust generation in a
    converter with minimum slag. ISIJ Int 29:291–299
Turkdogan ET, Leake LE (1959) Preliminary studies on the evolution of fumes from iron at high
    temperatures. J Iron Steel Inst 192:162–170
U.S. Environmental Protection Agency (1985) Locating and estimating air emissions from sources
    of manganese, U.S. EPA Report No. EPA-450/4-88-007h
Vasu A (2006) RTI report, U.S. Environmental Protection Agency, pp 36–50
Westfall LA, Cramer MH, Davourie J, McGough D, Ali M (2015) In: 14th International Ferroalloy
    Congress, INFACONXIV, Ukraine, pp 626–635
Zhang Y, Fruehan RJ (1995) Effect of the bubble size and chemical reactions on slag foaming.
    Metall Mater Trans B 26B:803–812